Corrosion Behavior of Ni-Cr Based Coatings in Simulated Human Body Fluid Environment

C.D. Arrieta-González[1,2], J. Porcayo-Calderon[3] , V.M. Salinas-Bravo[3], J.G. Chacon-Nava ,[1] A. Martinez-Villafañe[1], J.G. Gonzalez-Rodriguez[4]*

[1] Centro de Investigación en Materiales Avanzados, Miguel de Cervantes 120, 31109-Chihuahua, Chihuahua, MEXICO.
[2] Instituto Tecnológico de Zacatepec, Depto. De Ingeniería Química y Bioquímica, Av. Instituto Tecnológico 27, Zacatepec, Morelos, MEXICO
[3] Instituto de Investigaciones Eléctricas, Gerencia de Materiales y Procesos Químicos, Av. Reforma 113, Col. Palmira, 62490-Cuernavaca, Morelos, MEXICO.
[4] Centro de Investigación en Ingeniería y Ciencias Aplicadas-UAEM, Av. Universidad 1001, Col. Chamilpa, 62210-Cuernavaca, Morelos, MEXICO.
[*]E-mail: ggonzalez@uaem.mx

Potentiodynamic polarization and linear polarization resistance electrochemical techniques were used to assess the corrosion behavior of Ni20(% wt.)Cr, NiCrAl, NiCrAlY$_2$O$_3$, NiCrAlCoY$_2$O$_3$ and Cr$_2$C$_3$-Ni20Cr metallic coatings in simulated body fluid environment. Hank´s solution was used for simulating body fluid environment. Coatings were deposited on to AISI 304-type stainless steel by the High Velocity Oxygen Fuel (HVOF) system. All coatings were evaluated in the as deposited and grinded with 600 grade emery paper conditions. Corrosion behavior of all coatings was affected by both its chemical composition and surface finish. Scanning electron microscopy was used to observe the surface features of coatings before and after exposure in the corrosive media. Corrosion tests showed that by adding Al to the NiCr coating system in the as deposited condition decreased its corrosion potential whereas the corrosion current density (i_{corr}) increased in the order NiCrAl > NiCrAlYCo > Ni20Cr > NiCrAlY > Cr$_3$C$_2$(NiCr). Corrosion potential of coatings in the grinded condition nobler than coatings in the as coated condition whereas the i_{corr} value increased in the order NiCrAlY > NiCrAlYCo > NiCrAl > Cr$_3$C$_2$(NiCr) > Ni20Cr. The coating with the highest pitting potential value was NiCrAl, whereas the most susceptible to pitting type of corrosion was Cr$_3$C$_2$(NiCr). All coatings showed a crevice localized type of corrosion, and only NiCrAlY and Cr$_3$C$_2$(NiCr) coatings showed a repasivation, protection potential.

1. INTRODUCTION

Metals and alloys have been widely used in various shapes as implants in humans. They must have the required mechanical resistance and good corrosion resistance.

Corrosion and surface film dissolution are two responsible mechanisms for introducing ions in the body from the implants. Extensive release of metal ions from human body implants can result in adverse biological reactions and even lead to mechanical failure of the device. Most of the used materials for human implants include AISI 316L type stainless steels [1, 2], titanium-base alloys [3-7], or cobalt-base alloys [8-12]. These alloys can be used either as bulk materials or as coatings [13-17]. However, their main disadvantages are their high cost and lower wear resistance.

Ti-based alloys are considered to be good materials for implants because the passive film formed is not very reactive. In the passive state, these alloys are not completely stable and under certain circumstances the passive film breaks down producing localized corrosion. This fault calls to modify the material surface to increase the corrosion and wear resistance without affecting their mechanical properties [18].

Austenitic stainless steels, specially type AISI 316L is the most widely used steel for implants because of its low cost, easy to fabricate and welding if compared with Co-Cr and Ti alloys. 316L-type stainless steel has an acceptable corrosion resistance, biocompatibility, strength and fatigue resistance that makes it is a desirable material for surgical implants [19].

Because corrosion is the main issue related to failure of implants, an essential criterion for selection of alternative or new materials are the characteristics of the passive films formed, its mechanical properties and the bioactivity of the surface. This has come out in the proposal of new alloys with addition of nobler metals to replace the commonly used stainless steels or Ti-based alloys as well as the search for protective coatings.

The high cost of conventional materials used in implants has created interest for using surface treatments via deposition of coatings to improve the corrosion resistance of less costly materials that could be a substitute of conventional materials.

One of the methods for deposited metals that has gained interest is the thermal projection or high velocity oxygen-fuel (HVOF) method [20].

Adherence of coatings obtained by the HVOF process is mainly by mechanical keying and depends on the surface roughness. The HVOF technique significantly improves coating quality because the high kinetic energy of particles produces dense and adherent coatings in comparison to conventional plasma coatings [21].

Applied coatings by thermal projection consists of a wide family of coating systems which can cover a variety of materials. Fine particles are heated up to or close the melting point and sent out at high velocity to the substrate to produce a satisfactory bonding force.

These characteristics make that thermal projection be a one of the most versatile tools to achieve protection of materials [22]. Taking this premise as a starting point, in this work the corrosion resistance of Ni-Cr based coatings applied by the HVOF technique is investigated as an alternative for applications of biomaterials.

2. EXPERIMENTAL PROCEDURE

2.1. Tested coatings

A base coating with an 80(% wt.)Ni-20Cr chemical composition was selected. In order to observe the effect of different chemical elements on the base coating, NiCr coatings with addition of Al, Y, Co and chromium carbide were used. Table 1 shows the chemical composition of the different tested coatings.

Table 1 Chemical composition of tested coatings (% wt.).

Coating	Ni	Cr	Al	Y_2O_3	Co	Cr_3C_2
Ni20Cr	80	20				
NiCrAl	78.1	16.1	5.8			
NiCrAlY	60.9	28.2	9.9	1		
NiCrAlYCo	74	17.5	5.5	0.5	2.5	
Ni20Cr-Cr_3C_2	80	20				80

2.2. Coating procedure

The different coatings, except the Ni20Cr-Cr_3C_2 one, were applied on to 0.25 inches diameter AISI 304-type stainless steel rods (304SS) by thermal projection of fine particles using a Sultzer-Metco model 5PII system with oxyacetylene flame. In all cases, the same working conditions like distance of splaying, pressure and flow of gases was maintained for all coatings. The Ni20Cr-Cr_3C_2 coating was deposited by the supersonic HVOF method using a Sulzer Metco® model DJ2700 system with propane as fuel. The high velocity of particles in this method (> 500 m/s) and because of the high kinetic energy when they impact the substrate surface, produce coatings with high density and low porosity. Before coating, the rods were cleaned with acetone and their surface was shot blasted with alumina particles according to the NACE No.1/SSPC-SP 5 recommended practice [23]. After shot blasting, specimens were cleaned again with acetone and were ready for coating.

2.3. Electrochemical tests

Corrosion tests were carried out using two surface conditions: the as deposited and grinded with 600 grade emery paper. Coated rod specimens were casted in epoxy resin and electric contact was done by spot welding a Ni20Cr wire to one end of the specimen. Electrochemical tests were carried out using a three electrode electrochemical cell, with a saturated calomel electrode (SCE) as a reference electrode and a spiral wounded platinum wire as a counter electrode. All electrochemical tests were done with a fully computer controlled potentiostat from ACM instruments. The test media used in this work was in Hank´s solution. This solution was prepared with analytical grade components and distilled water with a final pH= 7.4. Table 2 shows the chemical composition of Hank´s solution.

Table 2. Hank´s solution chemical composition.

	NaCl	CaCl$_2$	KCl	NaHCO$_3$	Glucose	NaH$_2$PO$_4$	MgCl$_2$	Na$_2$HPO$_4$	MgSO$_4$
g/l	8.0	0.14	0.40	0.35	1.00	0.10	0.10	0.06	0.06

Throughout the tests a volume of 100 ml of nitrogen de-aerated Hank´s solution was used at a temperature of $37 \pm 1°C$. Before electrochemical tests, specimens were immersed during 60 min. in the test solution to allow for corrosion potential stabilization. Potentiodynamic polarization tests were done at a scanning rate of 0.166 mV/s in a -300 to +300 mV range versus the free corrosion potential, E_{corr}. Polarization resistance tests were done continuously for two weeks, taking one reading every 24 hr., by polarizing the specimen from -10 to +10 mV versus the E_{corr} value at a scanning rate was 0.166 mV/s. Pitting corrosion resistance was evaluated by anodic polarization according to ASTM F2120-01 and G3-89 standards. This test allows the free corrosion potential of the working electrode to stabilize during 1 hour and slowly scanning the potential in the anodic direction until a set potential value is reached; then the potential scan is reversed until a hysteresis loop closes [24]. The pitting or breakdown potential (E_b) is defined as the potential at which the pitting or crevice corrosion or both will initiate and propagate, and in the polarization curve appears as an abrupt increase in the anodic current density, at the point where the passive zone ends. An increase in the resistance to pitting corrosion is associated with a shift of E_b to nobler values. The protection potential (E_{pp}) is defined as the potential at which the forward and the reverse scans intersect. This value is always lower than the E_{np} value. After polarization tests specimens were analyzed in a DSM 960 Carl Zeiss scanning electronic microscope (SEM).

3. RESULTS AND DISCUSSION

3.1. Coating features

Fig. 1 shows a cross section of evaluated coatings. Figs. 1 a), b), c) and d) correspond to the coatings deposited by the thermal projection method. These coatings have the common features obtained by this process: they appear heterogeneous with a lamellar structure, low porosity, partially melted particles, partially fractured particles and the presence of embedded oxide within the coating. Fig. 1 e) corresponds to the coating deposited by the HVOF process. This process produces coatings of high density and porosity less than 1% [22]. The apparent porosity observed in this figure is due to the chromium carbide detachment during metallographic preparation of the specimen.

Coating adherence to the substrate is due mainly to mechanical forces. Fig. 2 shows the coating-substrate interface in both coating systems employed. In order to highlight the coating-substrate bond, the interface was etched. It can be seen that the first particles impacting the substrate surface were completely deformed and penetrated the surface imperfections, which guaranteed adequate adherence strength [25].
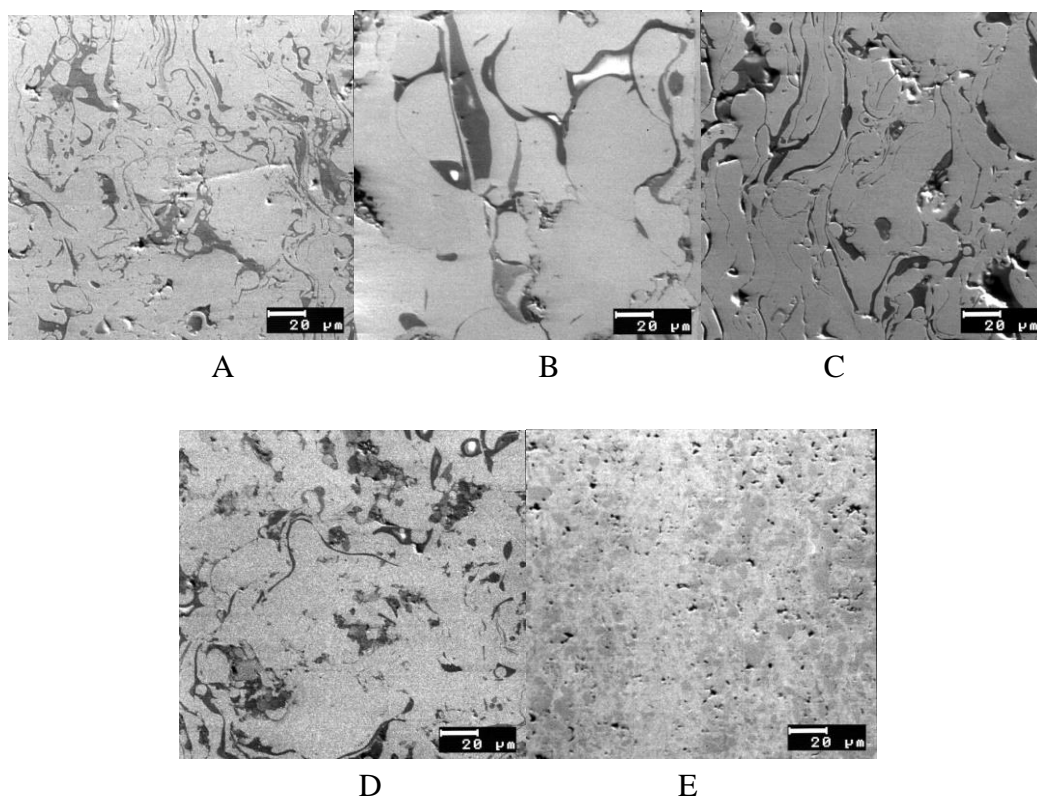
Figure 1. SEM micrographs of evaluated coatings showing the (a) Ni20Cr, (b) NiCrAl, (c) NiCrAlY, (d) NiCrAlYCo, (e) $Cr_3C_2(NiCr)$ coatings.
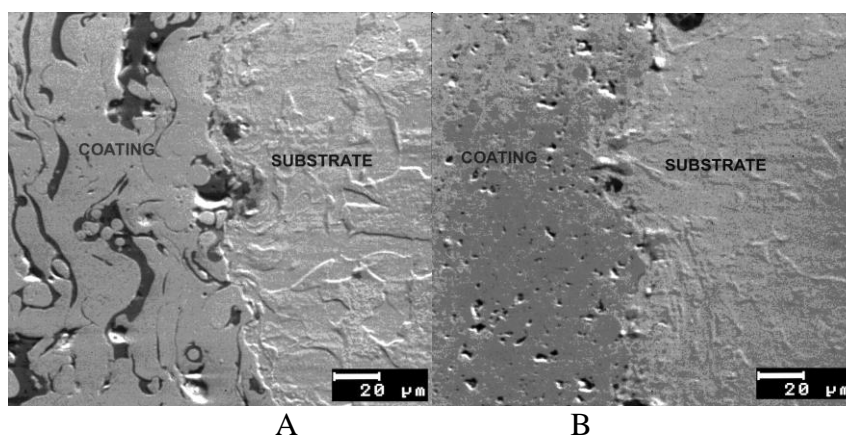
**Figure 2.** SEM micrographs showing the coating-substrate interfaces in the (a) NiCrAlY-304 SS, and (b) $Cr_3C_2(Ni20Cr)$-304 SS coating systems.

3.2. Potentiodynamic polarization tests.

Fig. 3 shows the polarization curves for the different coatings in the as deposited condition. It is observed that pitting corrosion potential varies with coating composition in the following way NiCrAl > Ni20Cr > NiCrAlYCo > NiCrAlY> $Cr_3C_2(Ni20Cr)$. According to the chemical composition of the

coatings, it can be observed that addition of Al to the NiCr coating system decreased its corrosion potential.
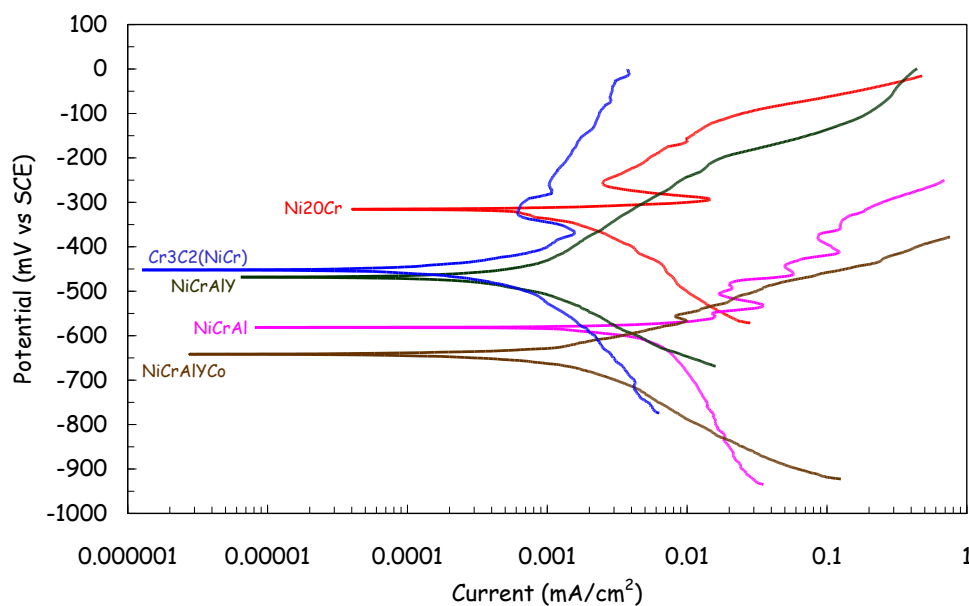
Figure 3. Polarization curves for the different coatings in the as deposited condition.

(a) Ni20Cr   (b) NiCrAl   (c) NiCrAlY

(d) NiCrAlYCo   (e) Cr$_3$C$_2$(Ni20Cr)
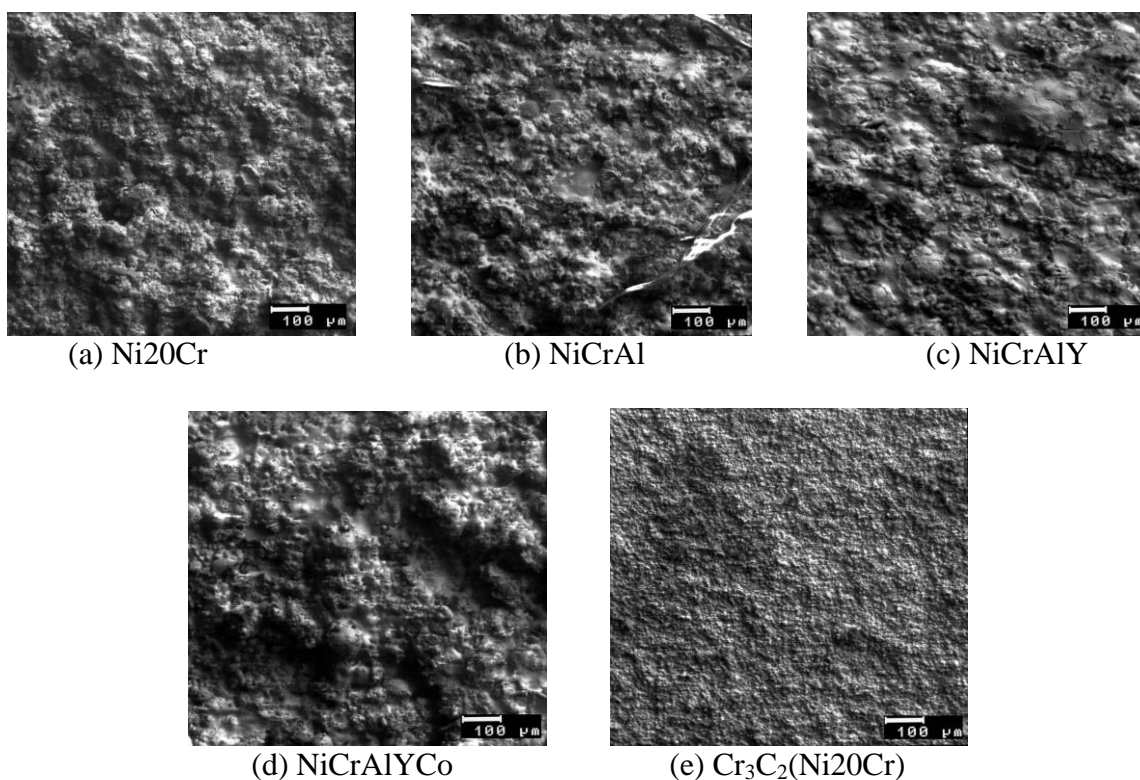
Figure 4. Surface features of coatings in the as deposited condition after polarization tests.

This is in agreement with studies on Al-rich coatings where it has been reported very negative values for the free corrosion potential value. This characteristic makes these coatings to be used as sacrificial coatings in salty environments [8]. Regarding the effect of other elements, it appears that they did not have a clear effect on the E_{corr} value. Corrosion current density values (i_{corr}) for the different coatings increased in the following order NiCrAl > NiCrAlYCo > Ni20Cr > NiCrAlY > Cr_3C_2(Ni20Cr). This behavior shows that the coating containing passive particles such as Cr_2Cr_3 showed the best corrosion resistance. This is because the Cr_3C_2(NiCr) coating is saturated with chromium carbide particles, however the coating surface of NICrAlY coating may have a higher aluminum oxide density produced during the coat process.

Fig. 4 shows the corroded surface of coatings after the polarization tests. In Figs 4 a)-d) it can be seen the characteristic features of coatings applied by the thermal projection process, whereas in Figs. 4 d the coatings applied by the HVOF process. After the polarization curves, the surface appears to have no great damage and it is notorious a great surface area because of surface irregularities. This fact indicates that the measured i_{corr} values obtained by taking into account the actual specimen area must be lower than the calculated ones because of the great surface area observed.

Fig. 5 shows the polarization curves of the different coatings in the grinded condition. Comparing Figs. 4 and 6 it can be seen that coatings in the grinded condition, except the NiCrAl and NiCrAlYCo, showed more active E_{corr} values than the corresponding values shown by the coatings in the as deposited condition. This can be explained because coatings in the as deposited condition have a larger oxidized surface. For the coatings in the grinded condition, the E_{corr} value varies in the following order: Ni20Cr > Cr_3C_2(NiCr) > NiCrAlY > NiCrAl > NiCrAlYCo. Essentially, they showed the same trend as the coatings in the as coat condition did, except the NiCrAl coating, probably associated with the presence of embedded oxides in the coating. All electrochemical parameters for the coatings in both the as-deposited and grinded conditions are summarized on table 3.

Table 3. Electrochemical parameters obtained from polarization curves for the as-deposited and grinded coatings.

	As-deposited		Grinded	
Coating	E_{corr} (mV)	I_{corr} (mA/cm^2)	E_{corr} (mV)	I_{corr} (mA/cm^2)
Ni20Cr	-310	2.5×10^{-3}	-410	3×10^{-4}
NiCrAl	-590	8×10^{-3}	-460	8×10^{-4}
NiCrAlY	-475	1×10^{-3}	-300	5×10^{-4}
NiCrAlYCo	-640	4×10^{-3}	-510	2×10^{-3}
Ni20Cr-Cr_3C_2	-450	8×10^{-4}	-560	1×10^{-3}

Corrosion current density values (i_{corr}) for grinded coatings varies as follows NiCrAlYCo > Cr_3C_2(NiCr) > NiCrAl > NiCrAlY > Ni20Cr. Compared to the as deposited condition, in this case the trend changed significantly. This change could be associated with the chemical stability that each coat

has. It can be considered that Ni20Cr coat is more stable and quickly develops a Cr_2O_3 protective film, the same apply to $Cr_3C_2(NiCr)$ besides the high density of passive carbide particles on it.
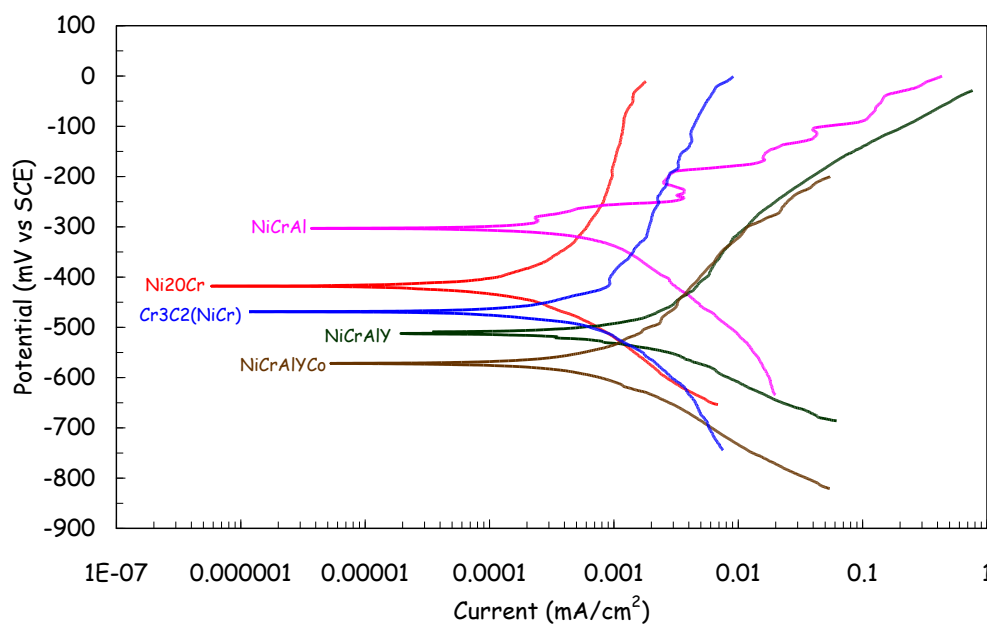
Figure 5. Polarization curves for coatings in the as grinded condition.

(a) Ni20Cr

(b) NiCrAl

(c) NiCrAlY

(e) $Cr_3C_2(Ni20Cr)$

(d) NiCrAlYCo
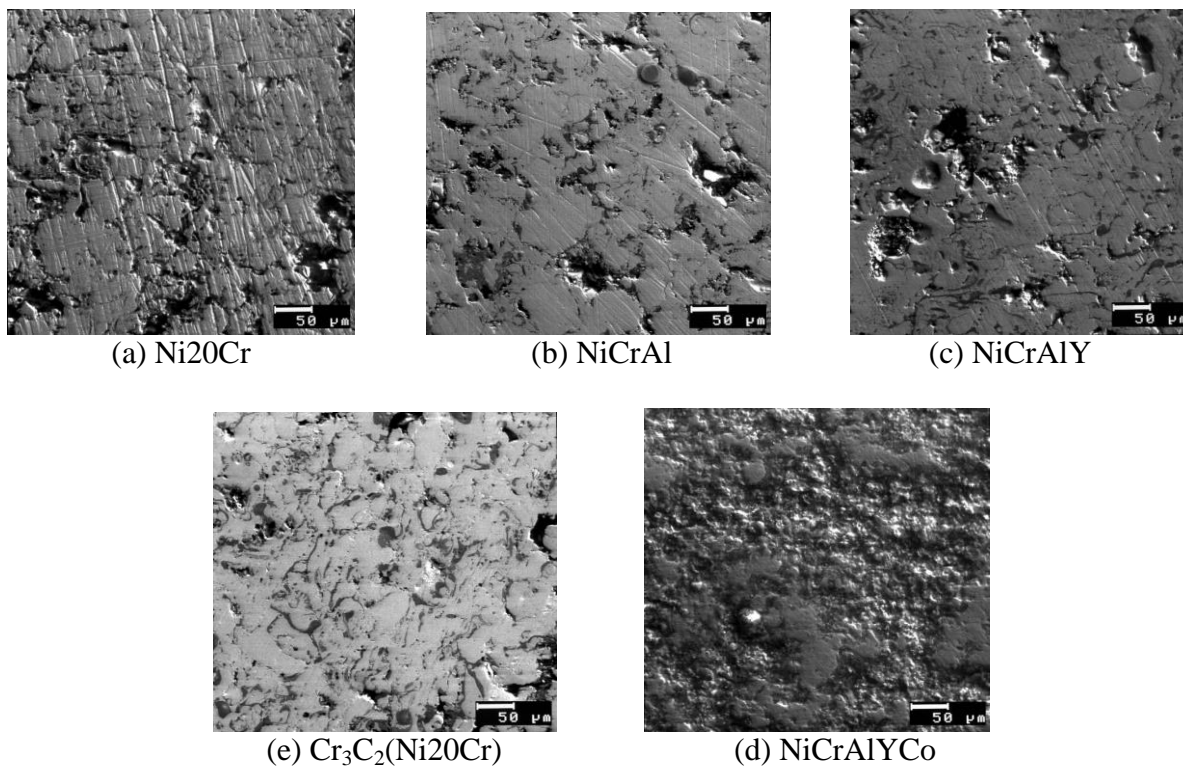
Figure 6. Surface features for coatings in the as grinded condition after polarization tests.

In the rest of coatings, because of lack of a pre-oxidized surface, a homogeneous distribution of Al particles favored a higher corrosion current density. This can be explained because powdered alloys employed to produce the investigated coatings are formed by NiCr particles and the rest of elements (Al, Co and Y_2O_3) are in the NiCr particles surface. When the particles are projected to the substrate, minor elements are partially incorporates to the main particle [4].

Morphological features of coatings in the grinded condition after polarization tests are shown on Fig. 6. In this case, all surfaces show some porosity reveled after the grinding process. Different contrast in the pictures is an indication of phases with different chemical composition. Pitting type of corrosion evidence was not observed after these tests.

3.3. Linear polarization resistance tests.

Fig. 7 shows the change in the i_{corr} value with time as obtained by the linear polarization tests after two weeks of testing.
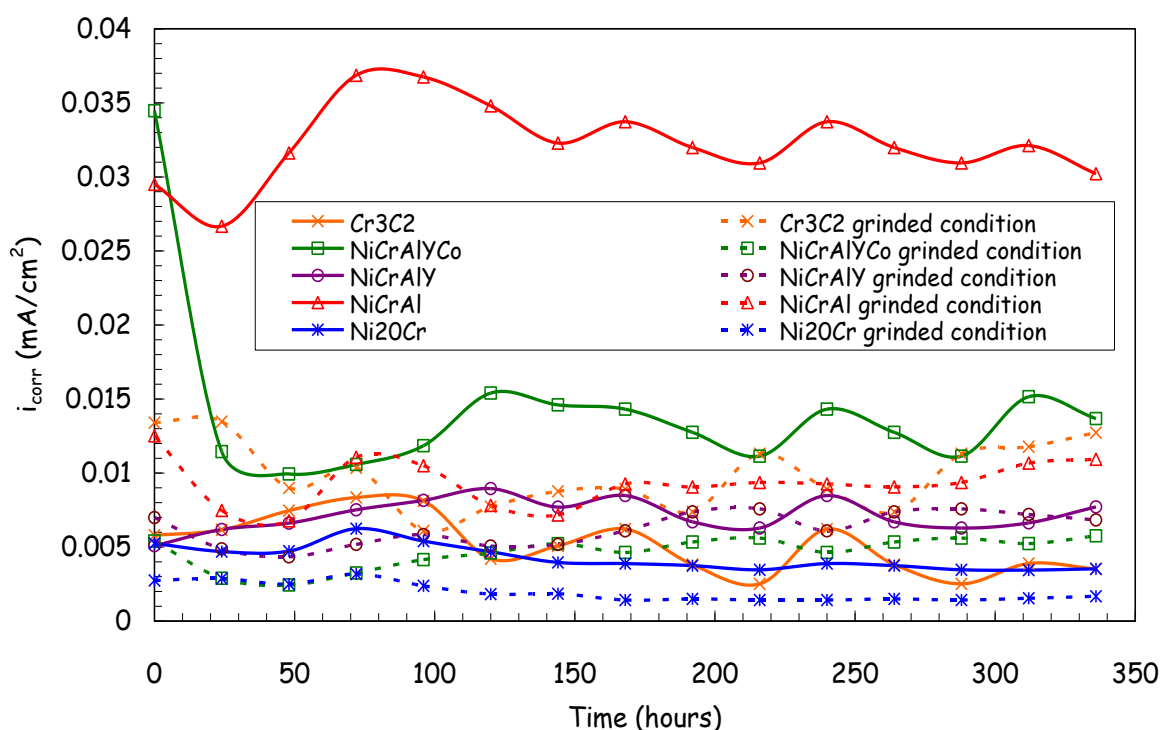

Figure 7. Change in the i_{corr} values with time for the different coatings after two weeks of testing

The highest corrosion rate was obtained for the as-deposited NiCrAl and NiCrAlYCo, whereas the lowest value, for more than one order of magnitude, was observed for the NiCr coatings in both the as-deposited and grinded conditions. It can also be observed that all coatings in the grinded condition showed lower i_{corr} values than the corresponding values obtained for the coatings in the as deposited condition. This behavior seems to be contradictory taking into consideration that coatings in as

deposited condition have a pre-oxidized surface condition; however this is justified because of the area effect of coatings in the grinded condition discussed above.

3.4. Pitting corrosion resistance tests.

The good corrosion behavior of these coatings might, however, be lost if for instance the passive film breaks down locally, giving rise to the formation of pits. Such susceptibility to pitting corrosion was evaluated by running cyclic polarization curves as shown on Fig. 8.
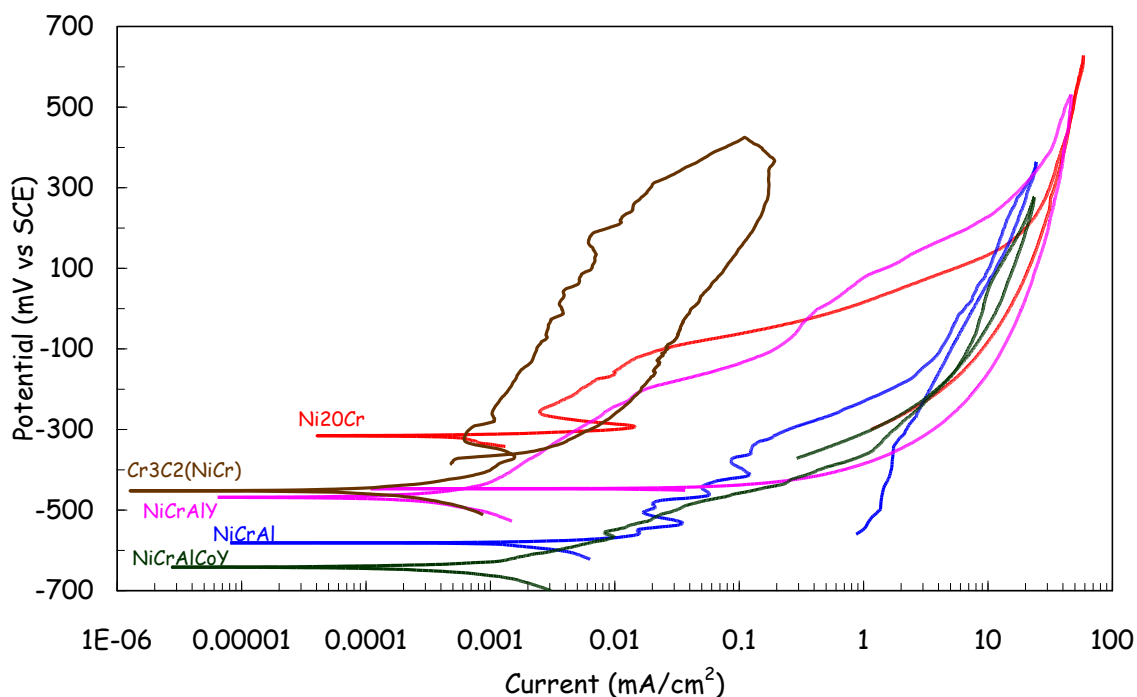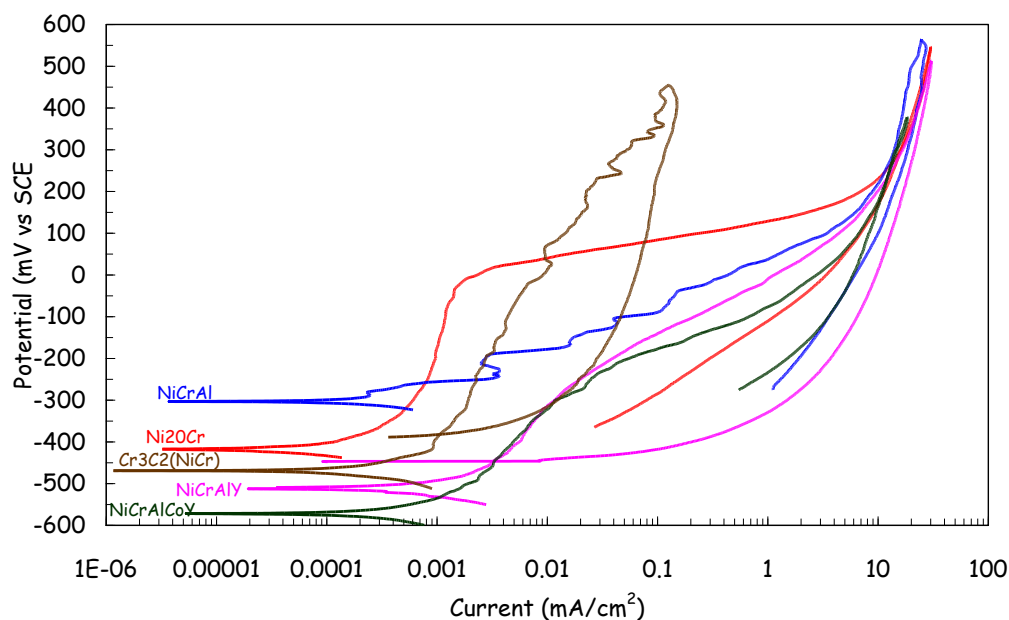

Figure 8. Pitting corrosion tests for coatings in the as deposited condition

Table 4. Fundamental parameters obtained from the cyclic polarization curves.

Coating	As-deposited			Grinded		
	E_{corr} (mV)	E_b (mV)	$E_b - E_{corr}$ (mV)	E_{corr} (mV)	E_b (mV)	$E_b - E_{corr}$ (mV)
Ni20Cr	-310	-100	210	-410	0	410
NiCrAl	-590	300	750	-460	260	720
NiCrAlY	-475	-350	240	-300	-200	100
NiCrAlYCo	-640	-200	275	-510	-220	290
Ni20Cr-Cr$_3$C$_2$	-450	-480	160	-560	-250	310

Only NiCrAlY and Cr$_3$C$_2$(Ni20Cr) showed a capacity for repassivation after pitting with a repassivation potential of -445 mV and -360 mV respectively, all other coatings did not show a repassivation potential. Pitting tests for coatings in the grinded condition showed the same behavior as tests in the as deposited condition as can be observed in Fig. 9. As in the deposited condition, only NiCrAlY and Cr$_3$C$_2$(Ni20Cr) coatings showed a repassivation potential of -445 mV and -380 mV respectively. The parameters of interest are given on table 4.

Figure 9. Pitting corrosion tests for coatings in the grinded condition

In general, the greatest the difference between the breakdown potential, E$_b$ and E$_{corr}$, give rise to the smallest pitting probability. Thus, this table shows that Cr$_3$C$_2$(Ni20Cr) coating, in both the as-deposited or grinded conditions, had the greatest difference between E$_b$ and E$_{corr}$, and, thus, the smallest pitting probability, followed by the NiCr and NiCrAlYCo coatings in the grinded condition. Therefore, NiCr coatings had the lowest corrosion rate and an acceptable pitting corrosion resistance, but by adding Cr$_3$C$_2$ this susceptibility to pitting corrosion and the capacity for repassivation substantially increased.

4. CONCLUSIONS

Surface characteristics had an influence on the corrosion behavior of coatings. Free corrosion potential values for the coatings in the as deposited condition were nobler than the corresponding values for coatings in the grinded condition. Increasing amounts of aluminum in the NiCr based coatings and addition of Cr$_3$Cr$_2$ with a pre-oxidized condition shifted the corrosion potential in the

active direction and decreased the corrosion current density, increasing, thus, the corrosion resistance of the coating. The same trend was obtained in coatings in the as grinded condition; however the corrosion current density in these coatings depends on the chemical stability of the coating in the electrolyte. The coating with the highest pitting potential value was NiCrAl, whereas the most susceptible to pitting type of corrosion was $Cr_3C_2(NiCr)$. Higher stability of coatings was obtained with Ni20Cr followed by $Cr_3C_2(NiCr)$ and lack of stability in all other coatings was due to an heterogeneous distribution of aluminum.

References

1. A.Choubey, B. Basu, R.Balasubramaniam, *Trends Biomater: Artif Organs* 18 (2005) 64.
2. T.M.Sridhar, U.K. Mudali, M.Subbaiyan, *Corros Sci* 45 (2003) 237.
3. Y.L. Zhou, M.Niinomi, T. Akahori, H.Fukui, H.Toda, *Mat Sci Eng* 398A (2005) 28.
4. R.W.Y. Poon, J.P.Y. Ho, X.Liu, C.Y. Chung, *Mat Sci Eng* 390A (2005) 444.
5. F.T. Cheng, K.H. Lo, H.C. Man, *J Alloys Compounds* 437 (2007) 322.
6. Y.F. Zheng, B.L. Wang, J.G. Wang, C.Li, L.C.Zhao, *Mat Sci Eng* 438A (2006) 891.
7. Y.H. Li, G.B. Rao, L.J. Rong, Y.Y. Li, W.Ke, *Mat Sci Eng 363A* (2003) 356.
8. M.Metikos-Hukovic, R.Babic, *Corros Sci* 49 (2007) 3570.
9. M.Metikos-Hukovic, R.Babic, *Corros Sci* 51 (2009) 70.
10. M.Clesic, W.Reczyski, A.M. Janus, K.Engvall, R.P. Socha, A.Kotarba, *Corros Sci* 51 (2009)1157.
11. J.H.Chern Lin, K.S. Chen, C.P. Ju, *Mat Chem Phys* 41 (1995):282.
12. W.Y. Guo, J. Surr, J.S. Wu, *Mat Chem Phys* 113 (2008):616.
13. Y. Cheng and Y.F. Zheng, *Surface and Coatings Technology* 201 (2007) 4909.
14. I.Gurapp, *Surface and Coatings Technology* 161 (2002) 4909.
15. Z.D. Cui, H.C. Man, X.J. Yang, *Surface and Coatings Technology* 192 (2005) 347.
16. Y.F. Cheng, X.L. Liu, H.F. Zhang, *Surface and Coatings Technology* 202 (2008) 3011.
17. Y.Q. Yang, H.C. Man, *Surface and Coatings Technology* 201 (2007) 6928.
18. H.S. Dobbs, *J. Mater. Sci*. 17 (1982) 2398.
19. U.K. Mudali, T.M. Sridhar, B. Raj, *Sadhana* 28, (2003) 601.
20. E. Lugscheider, P. Remer, A. Nyland, High velocity oxy fuel spraying: An alternative to the established APS-process for production of bioactive coatings, Surface modification technologies (ASM International) 2001.
21. L. Pawlowski, The Science and Engineering of Thermal Spray Coatings, John Wiley & Sons Ltd, (Second edition) 2008.
22. Joint Surface Preparation Standard NACE No. 1/SSPC-SP 5. White Metal Blast Cleaning.
23. S. Frangini, N. De Cristofaro, Corros Sci 45 (2003) 2769.
24. P.H. Suegama, C.S. Fugivara, A.V. Benedetti, J. Fernandez, J. Delgado, J.M. Guilemany, *Corros Sci* 47 (2005) 605.
25. T.C. Simpson, *Corrosion* 49 (1993) 550.